

1 **The biogeographic history of eelpouts and related fishes: linking phylogeny,**  
2 **environmental change, and patterns of dispersal in a globally distributed fish group**

3  
4 Scott Hotaling<sup>1,\*</sup>, Marek L. Borowiec<sup>2,\*</sup>, Luana S.F. Lins<sup>1,3</sup>, Thomas Desvignes<sup>4</sup>, and Joanna L.  
5 Kelley<sup>1</sup>

6  
7 **Affiliations:**

8 <sup>1</sup> School of Biological Sciences, Washington State University, Pullman, WA, USA

9 <sup>2</sup> Department of Entomology, Plant Pathology and Nematology, University of Idaho, Moscow, ID,  
10 USA

11 <sup>3</sup> Australian National Insect Collection, CSIRO, Canberra, ACT, Australia

12 <sup>4</sup> Institute of Neuroscience, University of Oregon, Eugene, OR, USA

13 \* Contributed equally

14  
15 **Correspondence:**

16 Joanna L. Kelley, School of Biological Sciences, Washington State University, Pullman, WA,  
17 99164, USA; Email: [joanna.l.kelley@wsu.edu](mailto:joanna.l.kelley@wsu.edu); Phone: (509) 335-0037

18  
19 **Declarations of Interest:** None

20  
21 **Abstract:**

22 Modern genetic data sets present unprecedented opportunities to understand the evolutionary  
23 origins of taxonomic groups comprising hundreds to thousands of species. When the timing of  
24 key events are known, it is also possible to investigate biogeographic history in the context of  
25 major phenomena (e.g., continental drift). In this study, we investigated the biogeographic  
26 history of the suborder Zoarcoidei, a globally distributed fish group that includes species  
27 inhabiting both poles and multiple taxa that produce antifreeze proteins to survive chronic  
28 subfreezing temperatures. We first generated a multi-locus, time-calibrated phylogeny for the  
29 group. We then used biogeographic modeling to reconstruct ancestral ranges across the tree  
30 and quantify the type and frequency of biogeographic events (e.g., founder, dispersal). With  
31 these results, we considered how the cooling of the Southern and Arctic Oceans, which reached  
32 their present-day subfreezing temperatures 10-15 million years ago (Mya) and 2-3 Mya,  
33 respectively, may have shaped the evolutionary history of Zoarcoidei, with an emphasis on the  
34 most speciose and widely distributed family, eelpouts (family Zoarcidae). Our phylogenetic

35 results clarified standing issues in the Zoarcoidei taxonomy and showed that the group began to  
36 diversify in the Oligocene ~31-32 Mya, with the center of origin for all families in north temperate  
37 waters. Within-area speciation was the most common biogeographic event in the group's history  
38 (80% of all events) followed by dispersal (20%). Finally, we found mixed evidence for polar  
39 ocean cooling underpinning Zoarcoidei diversification, with support limited to eelpout speciation  
40 in the Southern Ocean over the last 10 million years.

41

42 **Keywords:** phylogenetics, biogeographic modeling, biogeographic stochastic mapping,  
43 Southern Ocean, Antarctica, polar fish

44

#### 45 **1. Introduction:**

46 Clarifying spatial origins of diversification and the evolution of geographic ranges is key to  
47 understanding patterns of global biodiversity. By considering contemporary distributions in a  
48 phylogenetic context, it is possible to assess how key events (e.g., dispersal, extinction,  
49 speciation) shape range evolution and diversification (Dupin et al., 2017). With the ever-  
50 expanding availability of genetic data in public repositories (e.g., GenBank), declining costs for  
51 generating new data, and emerging statistical tools [e.g., biogeographic stochastic mapping  
52 (BSM), Matzke (2014)], there has never been a better time to explore complex biogeographic  
53 histories across large phylogenies. Cosmopolitan clades, where a single group is distributed  
54 throughout all or most of the world, present interesting biogeographical scenarios because no  
55 taxonomic group begins with a global distribution and thus many dispersal and vicariance  
56 events must occur during its evolution (Nauheimer et al., 2012). Moreover, long-term  
57 biogeographic shifts do not occur in an environmentally static landscape. While a group is  
58 evolving, diversifying, and shifting its range over millennia, the habitats it occupies are also  
59 changing in both size and suitability. Large-scale environmental shifts can drive species'  
60 radiations and when the timing of influential events (e.g., the separation of two land masses or  
61 cooling of a major ocean) are known, then it is possible to test hypotheses linking biogeographic  
62 patterns to processes on a calibrated timeline (Dupin et al., 2017).

63

64 A cosmopolitan group of particular biogeographical interest are eelpouts (family Zoarcidae), the  
65 most speciose family in the suborder Zoarcoidei, comprising ~75% of the suborder's ~400  
66 species (Fricke et al., 2018), and representing the only Zoarcoidei family with species that  
67 inhabit both poles (Møller et al., 2005). Eelpouts are also one of the most rapidly speciating fish  
68 clades, with their propensity for deep-waters and high-latitudes implicated as potential drivers of

69 their high speciation rate (Rabosky et al., 2018). At polar latitudes, marine environments are  
70 chronically cold, and often subfreezing, yet they retain high levels of biological productivity and  
71 species richness (DeVries and Steffensen, 2005). Considerable focus has been devoted to  
72 understanding how and when organisms diversified in the Southern and Arctic Oceans (e.g.,  
73 González-Wevar et al., 2010; Hopkins and Marinovich Jr, 1984), particularly as it relates to  
74 when both oceans reached their contemporary subfreezing temperatures [Southern Ocean: 10-  
75 15 million years ago (Mya), Arctic Ocean: 2-3 Mya; DeVries and Steffensen (2005)]. Generally  
76 speaking, most Zoarcoidei species are found in the Northern Hemisphere, specifically the  
77 northwestern Pacific Ocean, which has been proposed as a speciation center for the group  
78 (Anderson, 1994; Shmidt, 1950).

79  
80 A key innovation among the Zoarcoidei is the evolution of antifreeze proteins (AFP). AFPs have  
81 evolved repeatedly across the Tree of Life, including in multiple fish lineages beyond the  
82 Zoarcoidei (e.g., Antarctic notothenioids, Chen et al., 1997) and have been hypothesized to be a  
83 major factor underlying adaptive radiations in some groups (e.g., notothenioids, Matschiner et  
84 al., 2011). Adaptive radiations occur when high speciation rates, common ancestry, and a  
85 phenotype-environment correlation drive a rapid increase in species diversity and often stem  
86 from ecological opportunity (Schluter, 2000). For instance, the Antarctic notothenioid adaptive  
87 radiation into freezing Antarctic waters has been linked, in part, to the evolution of AFPs  
88 (Matschiner et al., 2011; Near et al., 2012). Within the Zoarcoidei, AFPs are present in at least  
89 five families—Anarhichadidae, Cryptacanthodidae, Pholidae, Stichaeidae, Zoarcidae (Davies et  
90 al., 2002; Davies et al., 1988)—with AFP-containing lineages inhabiting Arctic and Antarctic  
91 waters. Thus, the contemporary distributions of Zoarcoidei species, and particularly eelpouts  
92 living at both poles with their associated AFPs, raise questions about how cooling of the Arctic  
93 and Southern Oceans may have influenced the group's evolutionary history.

94  
95 Here, we used multi-locus sequence data to construct a time-calibrated, comprehensive  
96 phylogeny of the suborder Zoarcoidei. Next, we used this phylogeny to clarify issues of  
97 taxonomic uncertainty in the group and better understand its biogeographic history. To the first,  
98 previous phylogenetic efforts have noted issues with the Zoarcoidei taxonomy, primarily  
99 stemming from a lack of monophyly in the Stichaeidae family, which led to the description of two  
100 new families, Eulophiidae and Neozarcidae (Kwun and Kim, 2013). We confirm and build upon  
101 these prior efforts to improve Zoarcoidei taxonomy. To the second—biogeographic history—we  
102 reconstructed ancestral ranges for every node of our phylogeny and considered what, if any,

103 evidence exists for cooling of the Arctic and Southern Oceans to have driven patterns of  
104 speciation. We performed biogeographic stochastic mapping on our phylogeny to quantify the  
105 types of biogeographic events (e.g., founder-event speciation, dispersal) that have underpinned  
106 the group's diversification. To our specific question of whether ocean cooling has been a major  
107 driver of speciation within Zoarcoidei, and for eelpouts in particular since they are the only  
108 globally distributed family in the suborder, we expected to observe three lines of evidence: (1)  
109 higher support for biogeographic models that incorporate Arctic and Southern Ocean cooling,  
110 (2) bursts of speciation following the cooling of each ocean at roughly 10 (Southern) and 2  
111 (Arctic) Mya, and (3) more dispersal events into the Arctic and Antarctic than out of them as  
112 cold-adapted Zoarcoidei took advantage of new ecological opportunity.

113

## 114 **2. Materials and Methods:**

### 115 *2.1. Data collection*

116 We obtained sequence data for up to three nuclear genes (*rag1*, *rho*, *rnf213*) and three  
117 mitochondrial genes [*cytochrome oxidase I (mt-co1)*, *cytochrome B (mt-cyb)*, *16S rRNA (16S)*]  
118 from 223 specimens in the suborder Zoarcoidei and an outgroup, *Eleginops maclovinus*  
119 (suborder Notothenioidei). Our data set included a combination of existing data in GenBank and  
120 newly generated data (Table S1). For phylogenetic biogeographic modeling and ancestral range  
121 reconstruction (see *2.3 Biogeographic modeling and ancestral range estimation*), it was  
122 important that we binned species' contemporary distributions into geographic categories. We  
123 first defined the geographic distribution of each species in our data set using FishBase  
124 (<http://fishbase.org>; Froese and Pauly, 2019), an online database with species-level distribution  
125 information that stems from published literature and observations reported on the Ocean  
126 Biogeographic Information System (OBIS, <https://obis.org/>; Grassle, 2000) and the Global  
127 Biodiversity Information Facility (GBIF, <https://www.gbif.org/>; Lane and Edwards, 2007). We  
128 then binned contemporary distributions for each species into five geographic zones based on  
129 their latitudinal range with multiple zones allowed for a given taxon: (1) Arctic (north of the Arctic  
130 Circle, >66.5°N), (2) north temperate (23.5°N - 66.5°N), (3) tropical (between the Tropic of  
131 Cancer in the northern hemisphere and the Tropic of Capricorn in the southern hemisphere;  
132 23.5°N to 23.5°S), (4) south temperate (23.5°S - 66.5°S), and (5) Antarctic (south of the  
133 Antarctic Circle, >66.5°S).

134

135 We collected new sequence data for four species that were field-identified as *Ophthalmolycus*  
136 *amberensis*, *Lycenchelys tristichodon*, *Lycodapus endemoscotus*, and *Melanostigma* sp. using

137 polymerase chain reaction (PCR) and targeted Sanger sequencing. For each taxon, DNA was  
138 extracted from frozen tissue (either muscle, liver, or a fin clip) using a MagAttract HMW DNA Kit  
139 (Qiagen), following the manufacturer's protocol for 25 mg tissue samples. We amplified our six  
140 markers using primers listed in Table S2 with the same PCR conditions: initial denaturation for 4  
141 min at 94°C, 35 cycles of 30 s at 94°C, 30 s at 55°C and 45 s at 72°C, and a final elongation for  
142 7 min at 72 °C.

143  
144 We also extracted sequences for *Lycodichthys dearborni* (*rag1*, *rho*, *rnf213*, *mt-co1*, and *mt-*  
145 *cyb*) and *Lycodes polaris* (*rag1*, *rho*, *rnf213*, *mt-cyb*, and *16S*) from short-read genome  
146 assemblies. Genomes were assembled from high-coverage (>50x), short-read sequence data  
147 (either 100-bp or 150-bp paired-end Illumina sequence data) with SPAdes v3.11.1 and default  
148 settings (Bankevich et al., 2012). To extract sequences, we used BLAST+ v2.5.0 (Altschul et al.,  
149 1990) to align our primers against each assembly. Matches with an e-value less than 0.5 that  
150 were also the longest match between the query and target were identified as our best hits. We  
151 extracted the sequence between primers (the target) with bedtools (Quinlan and Hall, 2010). To  
152 confirm the identity of sequences, we used BLAST to compare the extracted markers against  
153 the NCBI database to verify they were similar to sequences from closely related species.

## 154 155 *2.2. Phylogenetic reconstruction and divergence timing*

156 Nucleotide sequences for *rag1*, *rho*, *rnf213*, *mt-co1*, and *mt-cytb* were translated to amino acid  
157 sequences and aligned using MUSCLE v3.8.31 with default settings (Edgar, 2004). Nucleotide  
158 alignments were then generated using the amino acid alignments with PAL2NAL v14-0  
159 (Suyama et al., 2006). Nucleotide sequences for *16S* were aligned using MUSCLE v3.8.31 with  
160 default settings (Edgar, 2004). After concatenation, we used the aligned nucleotide data set to  
161 estimate phylogeny using maximum likelihood and infer divergence times in a Bayesian  
162 framework. To infer the maximum likelihood tree we used IQ-TREE v1.6.10 (Nguyen et al.,  
163 2015). We provided partitions based on codon positions in each of the five coding genes and let  
164 each partition have an individual rate while sharing branch lengths across partitions (Chernomor  
165 et al., 2016). We let IQ-TREE find the best substitution models and partitioning scheme  
166 (Kalyaanamoorthy et al., 2017). To improve the thoroughness of the tree search algorithm we  
167 decreased the perturbation parameter to 0.3 from a default of 0.5 and increased unsuccessful  
168 tree search iterations to 500 from a default of 100. We assessed confidence across the tree with  
169 5,000 replicates of ultrafast bootstrap approximation (Hoang et al., 2018).

170

171 We estimated divergence timing under a fossilized birth-death process (Heath et al., 2014) as  
172 implemented in MrBayes v3.2.7a (Ronquist et al., 2012). We used the fossil *Proeleginops*  
173 *grandeastmanorum* (family Eleginopsidae, age 38-45 Mya) constrained as sister to the outgroup  
174 species *Eleginops maclovinus* (Bieńkowska-Wasiluk et al., 2013). Because of uncertainty of  
175 their placement, two fossil species—*Agnevicthys gretchinae* and *Palaeopholis laevis* (family  
176 Pholidae, age 11.5-12.3 Mya; Nazarkin, 2002)—were allowed to be placed as either the stem  
177 (outside of the clade formed by extant species) or crown (within the clade of extant species) for  
178 the group during exploration of the tree space. We included several fossils identified as  
179 Stichaeidae but because preliminary analysis demonstrated polyphyly of this family, we allowed  
180 these fossils to be placed anywhere within the in-group excluding Bathymasteridae: *Nivchia*  
181 *makushoki*, *Stichaeus brachigrammus*, and *Stichaeopsis sakhalinensis* (age 11.5-12.3 Mya;  
182 Nazarkin, 1998), undescribed fossils NSM PV 22683 (age 13-16 Mya) and PIN 3181/1050  
183 (11.6-13.5 Mya; Nazarkin and Yabumoto, 2015), and *Stichaeus matsubarai* (age 5.3-23 Mya;  
184 Yabumoto and Uyeno, 1994). We used fossils assigned to the contemporary species *Lycodes*  
185 *pacificus* (family Zoarcidae) to date its age at 0.78-2.59 Mya (Fitch, 1967).

186

187 For each fossil, we sampled age from a uniform distribution spanning its possible age range.  
188 Because recent work suggests gene-partitioning for divergence dating may result in  
189 unrealistically narrow confidence intervals (Angelis et al., 2018), we used an unpartitioned GTR  
190 model with gamma rate distribution broken into six discrete categories, the independent  
191 gamma-rate relaxed clock model, and extant sample proportion of 0.5. We set the root age prior  
192 to be an exponential distribution offset at 38 Mya (the youngest likely age of *P.*  
193 *grandeastmanorum*) with a mean of 70 Mya. We performed these analyses under two  
194 scenarios: one assuming taxon sampling was random and one assuming taxon sampling was  
195 done to maximize taxonomic diversity (Zhang et al., 2016). The choice of sampling scheme  
196 assumption can impact dating analyses if significant mismatch between assumed and actual  
197 taxon sampling exists. For example, when only a few species are sampled to represent genera  
198 or families in a clade containing thousands of species unequally distributed across these taxa,  
199 the sampling scheme is maximizing taxonomic and phylogenetic diversity and is different from a  
200 random sample of species from that clade. This can lead to bias in fossilized birth-death  
201 process dating (Zhang et al., 2016). For each MrBayes analysis we ran four replicates, each  
202 with four chains, for 400 million generations, sampling every 10,000 generations and discarding  
203 the first 20% of samples as burn-in. We assessed the reliability of these analyses by confirming  
204 that effective sample size for each parameter was greater than 100, potential scale reduction

205 factor values were close to 1.0, proposal acceptance rates were between 20-70%, average  
206 standard deviations of split frequencies were below 0.01, and that time-series of parameter  
207 values converged across replicates. We did not observe differences between random and  
208 diversified sampling. Thus, we used diversified sampling results for downstream analyses. To  
209 visualize summarize our results, we generated a lineages through time plot for the full species  
210 tree with the *ltt* function of Phytools (Revell, 2012) and plotting in ape (Paradis and Schliep,  
211 2019).

212

### 213 *2.3. Biogeographic modeling and ancestral range estimation*

214 For biogeographical modeling, we used “BioGeography with Bayesian (and likelihood)  
215 Evolutionary Analysis in R Scripts” v1.1.2 (BioGeoBEARS; Matzke, 2014). To identify the best-  
216 fit model, we compared likelihoods of six models for ancestral range estimation including  
217 dispersal-extinction cladogenesis (DEC; Ree, 2005; Ree and Smith, 2008), dispersal-vicariance  
218 analysis (DIVALIKE; Ronquist, 1997), and Bayesian inference of ancestral areas  
219 (BAYAREALIKE; Landis et al., 2013), as well as a variant of each model allowing for founder-  
220 event speciation (“+*j*” parameter designation). In addition to *j*, the models included two other free  
221 parameters: *d* (rate of range expansion) and *e* (rate of range contraction). Because our dated  
222 Bayesian consensus tree contained several polytomies, we ran BioGeoBEARS model selection  
223 separately on ten randomly chosen posterior trees to account for uncertainty. For all trees, we  
224 removed fossil taxa and taxonomic replicates to ensure that each species was represented only  
225 once. We also removed tips that were not reliably assigned to a described species (e.g., to  
226 genus only) and/or had no sampling locality information given and thus no geographic context.

227

228 After binning species into geographic zones as described above—Arctic, North Temperate,  
229 Tropical, South Temperate, Antarctic—we ran two types of BioGeoBEARS analyses. (1)  
230 “Unconstrained”, meaning dispersal probabilities were equal across time and space and taxa  
231 were allowed to have discontinuous ranges (e.g., Arctic and Tropical but not North Temperate).  
232 (2) A more parameter-rich and biologically realistic “time-stratified” analysis with dispersal  
233 probabilities modified for three pre-defined time periods—0-3 Mya, 3-20 Mya, and 20 Mya and  
234 older (i.e., the time before during and after cooling of the Arctic and Southern Oceans, DeVries  
235 and Steffensen, 2005)—to incorporate predicted geographic and ecological distances among  
236 range categories. Dispersal was penalized by distance only for the time period before the  
237 Southern or Arctic Oceans began cooling (>20 Mya), a dispersal penalty was added for the  
238 Antarctic zone after the Southern Ocean began cooling and reached its present state (3-20

239 Mya), and a dispersal penalty was added for the Arctic zone after the Arctic Ocean began  
240 cooling to its present-day temperature (0-3 Mya). For both sets of analyses, a maximum  
241 occupancy of three geographic zones was allowed and for the time-stratified analyses, only  
242 adjacent ranges were allowed (e.g., Tropical-North Temperate-Arctic). The dispersal matrices  
243 used in these analyses are provided in Table S3.

244

#### 245 *2.4. Biogeographic stochastic mapping*

246 In order to quantify the number of each type of biogeographic events in Zoarcoidei evolution we  
247 used biogeographic stochastic mapping (Dupin et al., 2017). Six types of biogeographic events  
248 were allowed in the models tested: speciation within-area (both species occupy the same area  
249 post-speciation), speciation within-area subset (one species inhabits a subset of the range post-  
250 speciation), vicariance, founder event, range expansion, and range contraction (see complete  
251 descriptions in Dupin et al., 2017). We differentiated among models using the Akaike  
252 information criterion corrected for small sample sizes (AICc; Cavanaugh, 1997). According to  
253 AICc, “BAYAREALIKE+J” was favored across all ten randomly selected posterior trees for both  
254 unconstrained and time-stratified analyses (see 3. Results). We therefore used  
255 BAYAREALIKE+J under the time-stratified regime for biogeographic stochastic mapping with  
256 100 stochastic replicate maps performed on each of the ten randomly chosen posterior trees.  
257 To obtain consensus results we averaged event counts from each of the 10 posterior trees for  
258 the best-fit model (BAYAREALIKE+J).

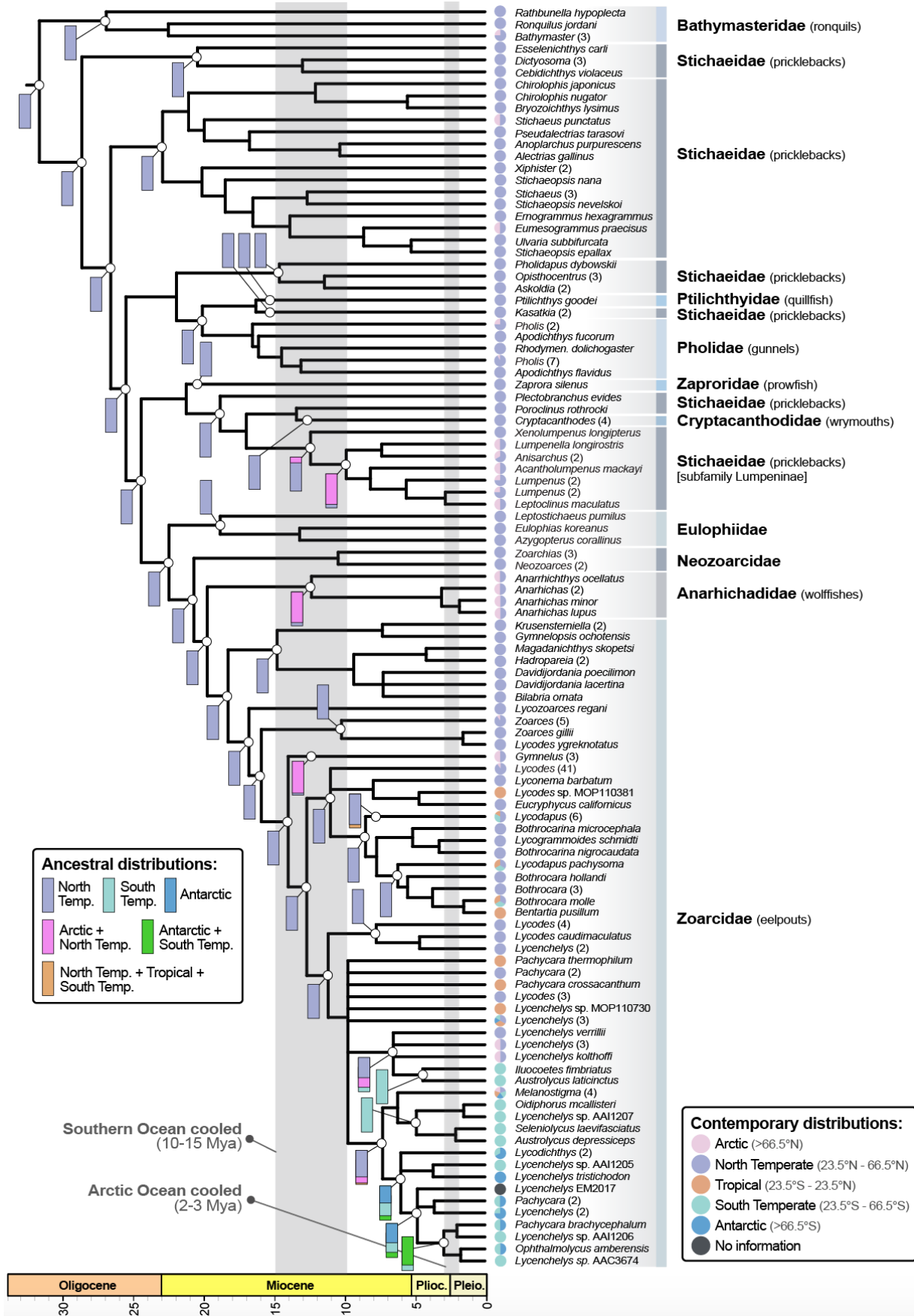
259

### 260 **3. Results:**

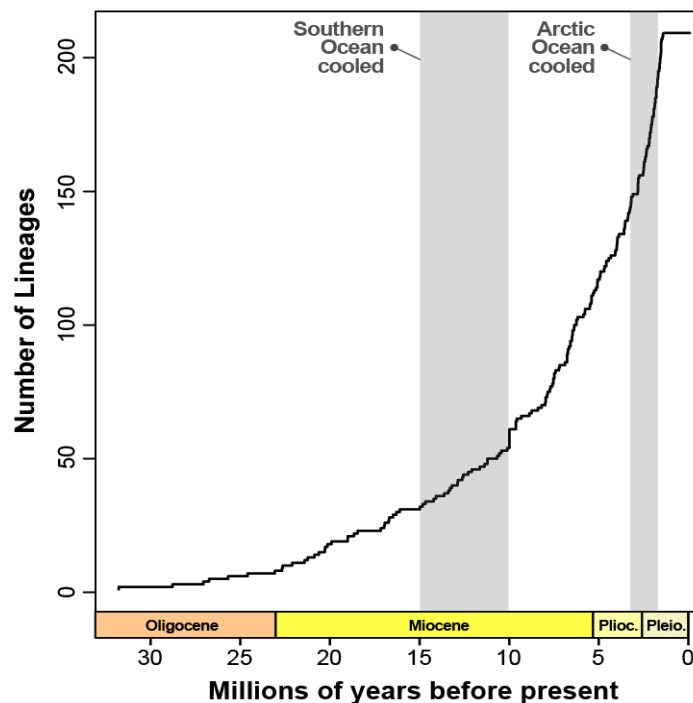
#### 261 *3.1. Data collection*

262 We acquired sequence data for 223 specimens representing at least 198 described species or  
263 subspecies from 10 families within Zoarcoidei. This translates to ~49% of described species  
264 diversity ( $n = 403$ ) in the suborder (FishBase; Froese and Pauly, 2019). For three families, we  
265 sampled 100% of described diversity: Anarhichadidae, Ptilichthyidae, and Zaproridae. For the  
266 most speciose family in the suborder—eelpouts (Zoarcidae)—we sampled 113 of 303 described  
267 species (37.3%; Figure 1). Across all specimens and markers, our data set was 44.9% complete  
268 with only seven (3.1%) specimens represented by a single marker. Sampled taxa spanned  
269 contemporary geographic zones with 42 species in the Arctic (15.1%), 180 species in the North  
270 Temperate zone (64.5%), 15 species in the Tropical zone (5.4%), 26 species in the South  
271 Temperate zone (9.3%), and 11 species in the Antarctic (3.9%; Table S1). Only eelpouts  
272 (Zoarcidae) had distributions in the South Temperate and Antarctic zones (Table S1).





274 **Figure 1.** A time-calibrated tree of the suborder Zoarcoidei. For visualization, when multiple species  
275 within the same genus formed a monophyletic group, we compressed the group. The number of taxa that  
276 were compressed are given in parentheses after the tip label. To the left of nodes, colored areas within  
277 vertical rectangles indicate the amount of support for that ancestral distribution group (Note: Up to three  
278 geographic zones could be combined for the ancestral range reconstruction). More area indicates more  
279 support for that ancestral distribution over others (if applicable). To the right of tips, small pie charts  
280 represent present-day distributions across our five latitudinally defined geographic zones (Arctic, North  
281 Temperate, Tropical, South Temperate, Antarctic). When multiple tips are compressed into one pie chart  
282 and/or a taxon's range spans multiple regions, the proportion for each region is reflected in the pie chart.  
283 Like historical distributions, contemporary distributions were also allowed to span more than one  
284 geographic zone. Thus, the number of pie chart components does not necessarily equal the number of  
285 taxa in a given group. The tree was rooted with *Eleginops maclovinus* which was removed for  
286 visualization. The numeric scale at the bottom of the figure indicates millions of years before present with  
287 corresponding geological epochs. Vertical gray bars indicate timing of the cooling of the Southern and  
288 Arctic Oceans, respectively. Complete trees (with outgroups) including dating estimates, probabilities for  
289 S1, S2, and S3, respectively.  
290  
291



292  
293 **Figure 2.** A lineage through time plot for the suborder Zoarcoidei with the timing of Southern and Arctic  
294 Ocean cooling noted.  
295

### 296 3.2. Phylogenetic reconstruction

297 Our phylogeny indicates that the Zoarcoidei diverged from the last common ancestor of  
298 notothenioids and Zoarcoidei during the Lower Cretaceous period, ~104 Mya [95% highest  
299 posterior density (HPD): 72-152 Mya] and began to radiate in the Oligocene, ~31-32 Mya  
300 (Figures 1, S1). Major families were recovered as monophyletic except for the Stichaeidae  
301 which were recovered as polyphyletic, in line with previous studies (e.g., Clardy, 2014;

302 Radchenko, 2016). Our results lend support to the current taxonomy of Eulophiidae and  
303 Neozoarcidae which were described by Kwun and Kim (2013) and expanded by Radchenko  
304 (2015). We also found support for the genus *Kasatkia* (currently in the Stichaeidae family) as  
305 sister to *Ptilichthys goodei*, the only described species in the family Ptilichthyidae (Figure 1).  
306 From a timing perspective, the eelpouts (Zoarcidae), the only family with a global distribution,  
307 emerged in the early Miocene (~18 Mya) and have steadily diversified until the present, with  
308 only one potential burst of speciation: the largest polytomy in our tree, suggesting rapid  
309 speciation, occurred ~10 Mya when the Southern Ocean had largely cooled to present-day  
310 temperatures (Figures 1-2).

311

312 **Table 1.** A summary of biogeographic model selection for the time-stratified analyses averaged across 10  
313 randomly selected posterior trees to account for polytomies in the consensus tree. Complete model  
314 selection results, including those for the “unconstrained” analyses which closely align with those  
315 presented here, are included in Table S4. The models tested follow those outlined in (Matzke, 2013) and  
316 include dispersal-extinction cladogenesis (DEC; Ree, 2005; Ree and Smith, 2008), dispersal-vicariance  
317 analysis (DIVALIKE; Ronquist, 1997), and Bayesian inference of ancestral areas (BAYAREALIKE; Landis  
318 et al., 2013) as well as a variant of each allowing for founder-event speciation (+j).

| Model         | Parameters | Mean AICc | $\Delta$ AICc | Model choice |
|---------------|------------|-----------|---------------|--------------|
| DEC           | 2          | 669.2     | 99.2          | 3            |
| DEC+j         | 3          | 645.2     | 75.2          | 2            |
| DIVALIKE      | 2          | 721.5     | 151.4         | 6            |
| DIVALIKE+j    | 3          | 684.8     | 114.8         | 5            |
| BAYAREALIKE   | 2          | 676.8     | 106.8         | 4            |
| BAYAREALIKE+j | 3          | 570.1     | --            | 1            |

319

### 320 3.3. Biogeographic modeling and ancestral range estimation

321 For both time-stratified and unconstrained analyses, our model selection results strongly  
322 favored the BAYAREALIKE +j model with the second-best model (DEC+j) 75 AICc units higher in  
323 both cases (Table 1). In line with similar biogeographic studies on cosmopolitan species (e.g.,  
324 Dupin et al. 2017), the inclusion of a founder-event speciation parameter (+j) substantially  
325 improved fit across all models tested (Tables 1, S4). Our time-stratified analyses were also a  
326 better fit to the data with a 31 AICc unit difference between the best-fit model (BAYAREALIKE +j)  
327 for time-stratified versus unconstrained analyses (Table S4). Given this, we focus hereafter on  
328 the time-stratified results. Ancestral range reconstruction under the best-fit model  
329 (BAYAREALIKE +j) supported a North Temperate origin for the entire suborder, as well as every  
330 family within the group with the exception of the wolffishes (family Anarhichadidae) with the bulk  
331 of support (>80%) in favor of a combined Arctic+North Temperate ancestral range for that group  
332 (Figure 1). Two other clades, one including Stichaeidae lineages with four *Lumpenus* species  
333 and the other containing three *Gymnelus* eelpout species, also exhibited strong support for an

334 Arctic+North Temperate origin. The only non-Northern Hemisphere ancestral range we found  
335 support for was within eelpouts, specifically a number of lineages in the subfamily Lycodinae.  
336 For example, for a clade containing several *Lycenchelys* and four *Lycodichthys* species,  
337 including *Lycodichthys dearborni*, an Antarctic resident known from 72°-78°S, we found ~50%  
338 support for an Antarctic ancestral range followed by ~40% support for South Temperate, and  
339 10% support for a combination of Antarctic+South Temperate (Figure 1).

340

341 **Table 2.** Summary of biogeographic stochastic mapping results for the suborder Zoarcoidei and the best-  
342 fit model (BAYAREALIKE+). The six types of biogeographic events allowed in the model are described  
343 fully in Dupin et al. (2017). Speciation within-area and speciation within-area subset differ in that under  
344 the former, ranges before and after divergence are the same whereas in the latter, one of the new  
345 lineages only occupies a subset of its former range. Included values are averaged [with standard  
346 deviations (SD) for the means] across 10 randomly selected posterior trees to account for polytomies in  
347 the consensus tree.

| Mode                   | Type                          | Mean (SD)   | Percent |
|------------------------|-------------------------------|-------------|---------|
| Within-area speciation | Speciation within-area        | 194.1 (1.4) | 80      |
|                        | Speciation within-area subset | 0           | 0       |
| Dispersal              | Founder event                 | 15.9 (1.4)  | 6.5     |
|                        | Range expansions              | 32.7 (2.4)  | 13.5    |
|                        | Range contractions            | 0           | 0       |
| Vicariance             | Vicariance                    | 0           | 0       |
| Total                  |                               | 241.7 (2.4) | 100     |

348

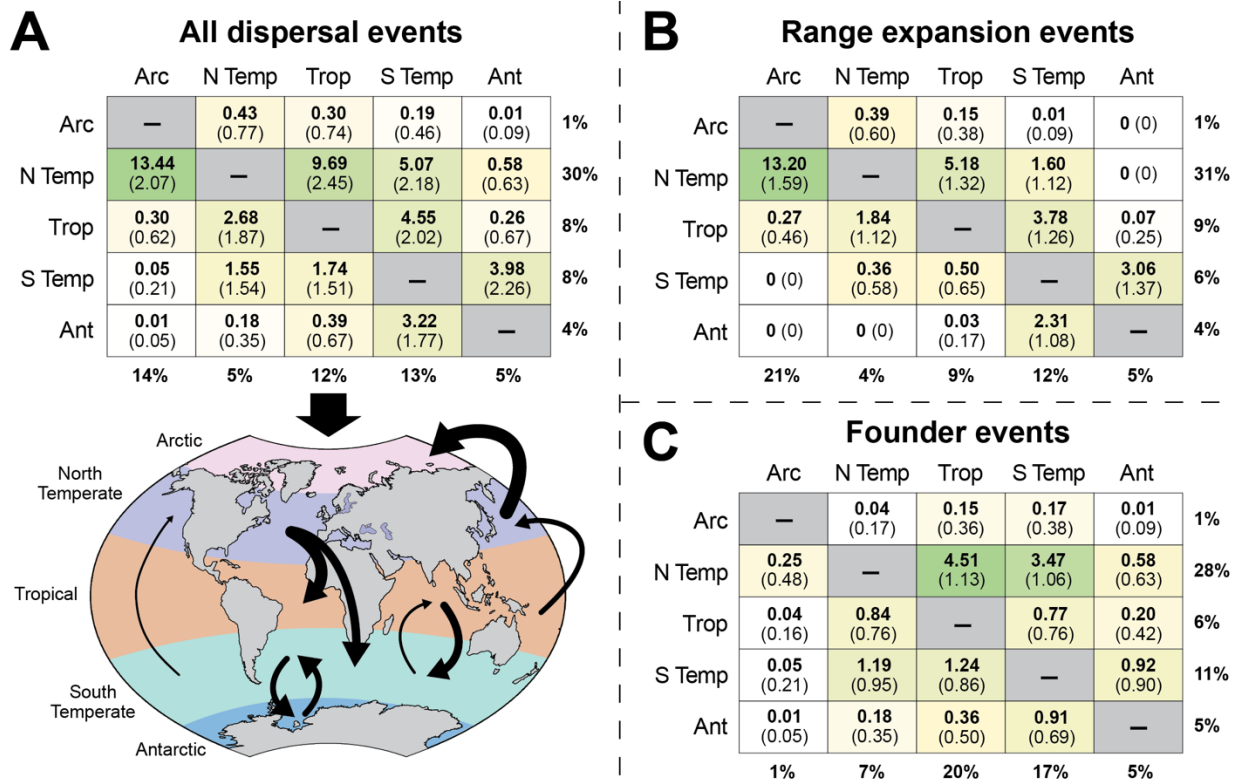
### 349 3.4. Biogeographic stochastic mapping

350 Across the Zoarcoidei, most biogeographic events were within-area speciation (80%) followed  
351 by two types of dispersals: range expansions (13.5%) and founder events (6.5%; Table 2). The  
352 fact that we observed a high number of within-area speciation events is unsurprising given that  
353 we divided the Earth into five large geographic zones. Similarly, a lack of vicariance events  
354 likely reflects the continuous nature of the marine environment with few strong dispersal  
355 barriers.

356

357 For dispersal events (i.e., range expansions and founder events), 30% of all events were out of  
358 the North Temperate zone with the bulk going into the adjacent Arctic (mean = 13.44 events) or  
359 Tropical (9.69) zones (Figure 3A). In general, far fewer dispersal events occurred in the  
360 Southern Hemisphere, likely reflecting how much more common Zoarcoidei species are in the  
361 Northern Hemisphere, and the North Temperate zone in particular (Figure 1). Range expansion  
362 events largely mirrored total dispersal events, with the bulk occurring from North Temperate into  
363 the Arctic zone (13.20; Figure 3B). Founder events, however, followed a slightly different pattern  
364 with most events occurring from the North Temperate into the Tropical (4.51) and South

365 Temperate (3.47) zones, respectively (Figure 3C). Again, this pattern likely reflects the  
 366 concentration of Zoarcoidei species in the North Temperate zone (Figure 1).  
 367  
 368 Focusing on the Arctic and Antarctic zones which cooled to their present-day subfreezing  
 369 temperatures over the last ~20 Mya, we observed asymmetric dispersal rates for both. Indeed,  
 370 just 1% of all dispersal events originated from the Arctic whereas it received 14% of all  
 371 dispersals. The Antarctic zone was less skewed but still showed a slight bias with 4% of all  
 372 dispersal events originating from it while receiving 5% (Figure 3). Collectively, most of the  
 373 asymmetry we observed was driven by range expansions into and out of the Arctic; the Arctic  
 374 received 21% of all range expansions while generating just 1% from within.  
 375



376  
 377 **Figure 3.** Summary of dispersal events in the history of the Zoarcoidei as estimated with biogeographic  
 378 stochastic mapping (BSM). Counts of dispersal events (bold) and standard deviations (in parentheses)  
 379 were averaged across 50 replicate BSMs for each of 10 phylogenies that were randomly sampled from  
 380 the posterior distribution. (A) Total dispersal events are given in the matrix and are depicted on a global  
 381 map with colors representing defined geographic zones. Black arrows between areas indicate the  
 382 frequency and direction of dispersal events. Only events with total mean counts of 1 or more are shown.  
 383 For visualization, arrow thickness corresponds to the  $\log_{10}$  of the event count multiplied by 2. Arrows only  
 384 correspond to individual geographic zones and do not correspond to specific oceans or regions. Their  
 385 placements within zones are purely for visualization. Total event counts in (A) are divided into the two  
 386 non-zero types of dispersal events observed in this study in (B) and (C). In (B) and (C), summarizing  
 387 percentages were calculated for each group separately so cannot be compared between them. Total

388 event counts, however, can be directly compared and sum to the values in (A). Within matrices, color  
389 indicates event frequency with darker green shading indicating higher frequencies. Given the counts and  
390 associated standard deviations, lower frequency counts (e.g., less than 1) are not necessarily different  
391 from zero. For each matrix, rows represent ancestral states where the lineage dispersed from and  
392 columns represent descendant states where the lineage dispersed to. The percentage of total events that  
393 a row or column comprises in a given matrix are shown in bold font on the margins. Geographic zone  
394 abbreviations include Arctic (Arc), North Temperate (N Temp), Tropical (Trop), South Temperate (S  
395 Temp), and Antarctic (Ant).  
396

#### 397 **4. Discussion:**

398 Our phylogenetic and biogeographic analyses confirmed that the suborder Zoarcoidei primarily  
399 evolved in northern temperate waters (23.5°-66.5°N). This general pattern is true for all families  
400 with one exception—the eelpouts (family Zoarcidae)—which exhibit a global distribution with a  
401 portion of their species diversity occurring from the Tropics to the Southern Ocean (Figure 1).  
402 Our best-fit biogeographic model included time-stratified matrices that reflected the elevated  
403 dispersal challenges of the Arctic and Southern Oceans as they cooled to their contemporary  
404 subfreezing temperatures. Support for these time-stratified analyses over models without time-  
405 stratification suggests that cooling of both oceans is important to understanding dispersal  
406 among the Zoarcoidei. We also observed a clear skew in dispersal directionality during the  
407 group’s evolutionary history with both range expansion and founder events much more likely to  
408 originate from the North Temperate zone than anywhere else. Finally, we confirmed standing  
409 issues with the Zoarcoidei phylogeny, namely a lack of monophyly for Stichaeidae, and we  
410 make recommendations to improve these issues below.

##### 411 412 *4.1. Phylogenetic reconstruction and biogeography*

413 Our analyses support diversification of families within the Zoarcoidei occurring ~31-32 Mya  
414 during the Oligocene, beginning with the separation of ronquils (family Bathymasteridae) from  
415 the rest of the group. This timing differs from two previous estimates but is closer to the ~37  
416 Mya estimate from Betancur-R et al. (2013) than the ~18 Mya estimate of Radchenko (2016),  
417 despite using the same markers as Radchenko (2016). In general, all divergences in our  
418 reconstruction were deeper in time than those of Radchenko (2016). Betancur-R et al. (2013)  
419 included many more taxa and calibrations than Radchenko (2016) and our data set included  
420 roughly three times as many specimens.

421  
422 From an ecological standpoint, the difference between the timing of eelpout (family Zoarcidae)  
423 emergence between our study (~18 Mya) versus the ~11-13 Mya reported by Radchenko  
424 (2016) is important as it places the group’s initial divergence on either side of when the

425 Southern Ocean reached its present-day subfreezing temperature 10-15 Mya (Figure 1).  
426 Eelpouts, as well as other high-latitude fish clades (e.g., Antarctic notothenids), are one of the  
427 fastest speciating fish groups (Rabosky et al., 2018). Thus, it is possible that the cooling of the  
428 polar seas, paired with key innovations like the evolution of AFPs (Deng et al., 2010), provided  
429 the necessary ecological opportunity and physiological tools necessary for two bursts of eelpout  
430 speciation as the Southern and Arctic Oceans cooled. We found some, albeit limited, evidence  
431 for this among southern lineages, with a multi-tip polytomy at 10 Mya, soon after the Southern  
432 Ocean reached its contemporary subfreezing conditions (Figures 1-2). This finding—  
433 diversification since the Southern Ocean reached its contemporary subfreezing temperature—  
434 generally aligns with findings for the Antarctic notothenioids (Near et al., 2015; Near et al.,  
435 2012). We saw less evidence for similar influence by Arctic Ocean cooling. A lack of influence  
436 by Arctic Ocean cooling on the evolutionary history of the Zoarcoidei could stem from the  
437 comparatively less harsh summer conditions of the Arctic versus Southern Ocean (e.g., water  
438 temperatures that are several degrees above zero, DeVries and Steffensen, 2005) reducing the  
439 ecological space for diversification (e.g., warmer water reducing the advantage of freezing  
440 tolerance), the more extreme physical isolation of the Southern Ocean relative to the Arctic  
441 Ocean, the more recent nature of Arctic cooling, or a combination of these, and perhaps other,  
442 factors.

443  
444 In terms of topology, our phylogeny aligns with related efforts (Betancur-R et al., 2013; Kwun  
445 and Kim, 2013; Radchenko, 2016; Radchenko, 2015) and confirms standing taxonomic issues  
446 for the Zoarcoidei that have been noted previously (Kwun and Kim, 2013; Radchenko, 2016).  
447 We observed a lack of monophyly within the pricklebacks (family Stichaeidae). In some  
448 instances, taxa that are considered Stichaeidae are sister to other families (e.g., the Stichaeidae  
449 genus *Kasatkia* and Ptilichthyidae, posterior probability  $\geq 0.95$ ; Figures 1, S2), highlighting the  
450 need for the continued re-evaluation of higher-level taxonomic assignments within the suborder.  
451 Kwun and Kim (2013) addressed two of these issues by establishing two new families—  
452 Eulophiidae and Neozoarcidae—and reclassifying species previously considered to be  
453 Stichaeidae and Zoarcidae within them. Radchenko (2016) expanded on these descriptions,  
454 finding support for additional species to be grouped within both families. Our results support  
455 these taxonomic changes as well. Still, because Stichaeidae appear to have acted—at least in  
456 part—as a taxonomic “catch all” for the suborder, issues remain. For instance, *Poroclinus*  
457 *rothrocki* is currently assigned to Stichaeidae but we recovered it as sister to  
458 Cryptacanthodidae. Similarly, we recovered *Plectobranthus evides* (currently Stichaeidae) as

459 sister to both *P. rothrocki* and *Zaprora silenus* (Zaproridae; Figure 1). Node probabilities for  
460 these three branches range from 0.61-0.85 (Figure S2) highlighting uncertainty around their  
461 placement. Thus, it is possible—and perhaps likely—that they each represent monotypic  
462 families similar to the prowfish (Zaproridae) but without additional analyses, ideally incorporating  
463 additional molecular data with morphological characters, it will remain uncertain. Finally, given  
464 monophyletic evidence in this study (posterior probability = 0.61; Figure S2) and the findings of  
465 Radchenko (2015), it may be warranted to elevate the subfamily Lumpeninae (Stichaeidae;  
466 Figure 1) to its own family, Lumpenidae.

467

#### 468 *4.2. Ancestral range estimations*

469 Over 70 years ago, Shmidt (1950) hypothesized that major families in the suborder Zoarcoidei  
470 evolved in the northern Sea of Okhotsk (~60°N) during the Miocene (23-5.5 Mya). In addition to  
471 our phylogenetic results supporting this timeline, our ancestral range reconstructions also  
472 supported it by showing that Zoarcoidei species largely diversified in mid-latitude regions of the  
473 Northern Hemisphere. In general, the ancestral range of a Zoarcoidei clade or lineage reflected  
474 its present-day distributions. This is particularly interesting in the context of eelpouts and their  
475 cosmopolitan distribution at both poles, the only family in the suborder to exhibit such a pattern  
476 (and one of only 10 families across all fishes, Møller et al., 2005). In addition to polar  
477 distributions, eelpouts are also the only Zoarcoidei family to commonly inhabit the deep sea (>  
478 1000 m) and occur near hydrothermal vents (Møller et al., 2005). A wide range in preferred  
479 depths has been proposed as one factor that enhances geographical range size in marine  
480 organisms (Brown et al., 1996). This may be particularly true for deep water species like  
481 eelpouts given that the deep sea, while extreme in terms of pressure, cold, and darkness, is  
482 more environmentally consistent than shallower habitats and has few impediments to dispersal  
483 (Gaither et al., 2016). Thus, the global distribution of eelpouts relative to other families in the  
484 suborder (as well as their exceptionally high speciation rate, Rabosky et al., 2018) may be due  
485 to deep sea habitat connectivity paired with a propensity for adapting to extremes, whether  
486 subfreezing waters (Deng et al., 2010) or hydrothermal vents (Machida and Hashimoto, 2002).

487

#### 488 *4.3. Directionality of dispersal events*

489 A striking biogeographic pattern within the Zoarcoidei is strong asymmetry in dispersal among  
490 geographic zones. For almost every pairing of geographic zones (e.g., Arctic and North  
491 Temperate), the rate of dispersal events was much higher from one zone into the other versus  
492 the reciprocal. This was most notable for the North Temperate zone, the center of origin for the



493 group according to ancestral range reconstructions. Dispersals out of the North Temperate zone  
494 accounted for 30% of all events while dispersals into it only accounted for 5% (Figure 3A).  
495 Similar patterns of asymmetric dispersal have been observed for other species, particularly from  
496 the North Pacific into the Arctic, for mollusks (Marincovich and Gladenkov, 1999) and other  
497 deep-water fishes (e.g., snailfishes, family Liparidae; Orr et al., 2019).

498  
499 We also observed differences in dispersal rates for the Arctic and Antarctic. Given a relatively  
500 less harsh barrier to dispersal for species into or out of the Arctic versus Antarctic waters, which  
501 are surrounded by the Antarctic Circumpolar Current (ACC) and an extreme temperature drop  
502 (Barker et al., 2007), we expected more bidirectional dispersal for Arctic versus Antarctic. Our  
503 results, however, did not fully align with this expectation; while dispersal into the Arctic is indeed  
504 common (14% of all events), dispersal out of the Arctic is extremely rare (~1%, Figure 3A). This  
505 starkly contrasts with the slightly higher but largely equivalent rates of dispersal into and out of  
506 the Antarctic (4% vs. 5% respectively, Figure 3A). Given the deep-water distributions of  
507 eelpouts and their tolerance for subfreezing temperatures, this result may be linked to  
508 differences in ecological opportunity or other factors between the regions. However, it might  
509 also simply reflect lineage age and species richness. The Arctic is adjacent to the North  
510 Temperate zone, the most likely center of origin for the group (and where much of its species  
511 richness remains), and by cooling much more recently, any barrier to dispersal that it presents  
512 are much younger than the Antarctic. Thus, a combination of geographic proximity to the  
513 Zoarcoidei center of origin paired with more recent thermal changes may be the most  
514 parsimonious explanation for the dispersal differences we observed between polar regions.

515

#### 516 *4.4. Potential caveats and future directions*

517 Integrating phylogenetic insight with historical biogeographic modeling is a powerful approach  
518 for understanding the evolutionary history of organismal groups. When paired with well-studied  
519 environmental events (e.g., ocean cooling, continental separation), hypotheses about the  
520 relative importance of those events can be tested in a statistically robust framework. Still, this  
521 approach, and our implementation, is not without caveats that should be considered when  
522 interpreting our results and considering future studies.

523

524 The total numbers of biogeographic events reported in this study represent minima as we  
525 sampled ~49% of the described species in the suborder. While more taxonomic sampling would  
526 provide greater resolution of the true value of these figures, it is unlikely to alter the relative

527 proportions of each since, to our knowledge, no major bias in our sampling scheme exists in  
528 terms of both taxonomic representation and geographic scope. However, this only applies to the  
529 currently described taxonomic diversity. A more general, and important, caveat lies in the lack of  
530 knowledge surrounding Zoarcoidei species. Both eelpouts and the broader suborder are  
531 relatively deep-water taxa, living in hundreds to thousands of meters of water, with little  
532 biomedical or economic benefit. As such, they are understudied, and this lack of natural history  
533 knowledge may bias our results in two ways. First, many Zoarcoidei species have been  
534 described from the Sea of Okhotsk off the southeastern coast of Russia (~55°N) and broadly  
535 from the Northern Hemisphere (Anderson, 1994). It is possible that a bias in both sampling  
536 effort and species descriptions towards the Northern Hemisphere, and specifically the North  
537 Temperate zone used in our study, influenced our results. However, our use of broad  
538 geographic zones likely tempered this effect as it allowed for broader distributions and therefore  
539 more uncertainty in species' ranges. Second, most Zoarcoidei species have been described  
540 from morphology alone (Anderson, 1994) and little to no molecular insight exists for the group  
541 beyond phylogenies that target single representatives for each clade. Given the propensity for  
542 cryptic diversity even in well-studied groups (e.g., mouse lemurs, Hotaling et al., 2016) and the  
543 potential for morphologically distinct animals to be the same species (e.g., Jones and Weisrock,  
544 2018), future efforts to assess species boundaries with molecular data across the suborder will  
545 improve resolution of their biogeographic history.

546

## 547 **5. Conclusion:**

548 In this study, we used a densely sampled, time-calibrated phylogeny of the suborder Zoarcoidei,  
549 with an emphasis on the globally distributed eelpouts, to understand evolutionary relationships  
550 and biogeographic history for the group. From a taxonomic standpoint, we highlighted existing  
551 issues with the Zoarcoidei taxonomy and proposed new solutions. For biogeography, while our  
552 analyses at large geographic scales yielded key insights for the suborder and major clades,  
553 more targeted analyses of individual families paired with finer-scale distribution information and  
554 molecular data, will allow for testing more specific biogeographic hypotheses. Similarly, future  
555 efforts to use the same biogeographic methods across multiple taxonomic groups, perhaps  
556 comparing eelpouts to other deep, cold-water fauna (e.g., snailfishes), could shed additional  
557 light on how generalizable the role of major environmental changes like ocean cooling has been  
558 for fish diversification.

559

560 **6. Acknowledgements:**

561 We acknowledge funding from the Antarctic Bursary, a Washington State University New  
562 Faculty Seed Grant, and NSF awards (OPP-1543383 and OPP-1947040 supporting T.D. and  
563 OPP-1906015 to J.L.K). We thank Keegan Paras and Charlotte Walker for their help with  
564 analyses. We also acknowledge the Computational Resources Core of the University of Idaho  
565 Institute for Bioinformatics and Evolutionary Studies (IBEST).

566

567 **7. Data statement:**

568 The data (including sequence alignments), code, and additional results for this study are  
569 publicly available on Zenodo (<https://doi.org/10.5281/zenodo.4306092>).

570

571 **8. References:**

- 572 Altschul, S.F., Gish, W., Miller, W., Myers, E.W., Lipman, D.J., 1990. Basic local alignment  
573 search tool. *Journal of Molecular Biology* 215, 403-410. [https://doi.org/10.1016/S0022-](https://doi.org/10.1016/S0022-2836(05)80360-2)  
574 [2836\(05\)80360-2](https://doi.org/10.1016/S0022-2836(05)80360-2)
- 575 Anderson, M.E., 1994. Systematics and osteology of the Zoarcidae (Teleostei: Perciformes).  
576 *Ichthyological Bulletin of the J.L.B. Smith Institute of Ichthyology* 60, 1-120.
- 577 Angelis, K., Álvarez-Carretero, S., Dos Reis, M., Yang, Z., 2018. An evaluation of different  
578 partitioning strategies for Bayesian estimation of species divergence times. *Systematic*  
579 *Biology* 67, 61-77. <https://doi.org/10.1093/sysbio/syx061>
- 580 Bankevich, A., Nurk, S., Antipov, D., Gurevich, A.A., Dvorkin, M., Kulikov, A.S., Lesin, V.M.,  
581 Nikolenko, S.I., Pham, S., Pribelski, A.D., 2012. SPAdes: a new genome assembly  
582 algorithm and its applications to single-cell sequencing. *Journal of Computational*  
583 *Biology* 19, 455-477. <https://doi.org/10.1089/cmb.2012.0021>
- 584 Barker, P.F., Filippelli, G.M., Florindo, F., Martin, E.E., Scher, H.D., 2007. Onset and role of the  
585 Antarctic Circumpolar Current. *Deep Sea Research Part II: Topical Studies in*  
586 *Oceanography* 54, 2388-2398. <https://doi.org/10.1016/j.dsr2.2007.07.028>
- 587 Betancur-R, R., Broughton, R.E., Wiley, E.O., Carpenter, K., López, J.A., Li, C., Holcroft, N.I.,  
588 Arcila, D., Sanciangco, M., Cureton li, J.C., 2013. The tree of life and a new  
589 classification of bony fishes. *PLoS currents* 5.  
590 <https://doi.org/10.1371/currents.tol.53ba26640df0ccaee75bb165c8c26288>
- 591 Bieńkowska-Wasiluk, M., Bonde, N., Møller, P.R., Gaździcki, A., 2013. Eocene relatives of cod  
592 icefishes (perciformes: Notothenioidei) from Seymour Island, Antarctica. *Geological*  
593 *Quarterly* 57, 567-582, doi: 510.7306/gq. 1112. <https://doi.org/10.7306/gq.1112>

- 594 Brown, J.H., Stevens, G.C., Kaufman, D.M., 1996. The geographic range: size, shape,  
595 boundaries, and internal structure. *Annual Review of Ecology and Systematics* 27, 597-  
596 623. <https://doi.org/10.1146/annurev.ecolsys.27.1.597>
- 597 Cavanaugh, J.E., 1997. Unifying the derivations for the Akaike and corrected Akaike information  
598 criteria. *Statistics & Probability Letters* 33, 201-208. [https://doi.org/10.1016/S0167-  
599 7152\(96\)00128-9](https://doi.org/10.1016/S0167-7152(96)00128-9)
- 600 Chen, L., DeVries, A.L., Cheng, C.H., 1997. Evolution of antifreeze glycoprotein gene from a  
601 trypsinogen gene in Antarctic notothenioid fish. *Proceedings of the National Academy of  
602 Sciences* 94, 3811-3816. <https://doi.org/10.1073/pnas.94.8.3811>
- 603 Chernomor, O., Von Haeseler, A., Minh, B.Q., 2016. Terrace aware data structure for  
604 phylogenomic inference from supermatrices. *Systematic Biology* 65, 997-1008.  
605 <https://doi.org/10.1093/sysbio/syw037>
- 606 Clardy, T.R., 2014. Phylogenetic systematics of the prickleback family Stichaeidae (Cottiformes:  
607 Zoarcoidei) using morphological data. Dissertations, Theses, and Masters Projects.  
608 1539616612. <https://doi.org/10.25773/v5-fyer-5n47>
- 609 Davies, P.L., Baardsnes, J., Kuiper, M.J., Walker, V.K., 2002. Structure and function of  
610 antifreeze proteins. *Philosophical transactions of the Royal Society of London. Series B,  
611 Biological sciences* 357, 927-935. <https://doi.org/10.1098/rstb.2002.1081>
- 612 Davies, P.L., Hew, C.L., Fletcher, G.L., 1988. Fish antifreeze proteins: physiology and  
613 evolutionary biology. *Canadian Journal of Zoology* 66, 2611-2617.  
614 <https://doi.org/10.1139/z88-385>
- 615 Deng, C., Cheng, C.H., Ye, H., He, X., Chen, L., 2010. Evolution of an antifreeze protein by  
616 neofunctionalization under escape from adaptive conflict. *Proceedings of the National  
617 Academy of Sciences of the United States of America* 107, 21593-21598.  
618 <https://doi.org/10.1073/pnas.1007883107>
- 619 DeVries, A.L., Steffensen, J.F., 2005. The Arctic and Antarctic polar marine environments. *Fish  
620 physiology* 22, 1-24. [https://doi.org/10.1016/S1546-5098\(04\)22001-5](https://doi.org/10.1016/S1546-5098(04)22001-5)
- 621 Dupin, J., Matzke, N.J., Särkinen, T., Knapp, S., Olmstead, R.G., Bohs, L., Smith, S.D., 2017.  
622 Bayesian estimation of the global biogeographical history of the Solanaceae. *Journal of  
623 Biogeography* 44, 887-899. <https://doi.org/10.1111/jbi.12898>
- 624 Edgar, R.C., 2004. MUSCLE: multiple sequence alignment with high accuracy and high  
625 throughput. *Nucleic acids research* 32, 1792-1797. <https://doi.org/10.1093/nar/qkh340>

- 626 Fitch, J., 1967. The marine fish fauna, based primarily on otoliths, of a lower Pleistocene deposit  
627 at San Pedro, California (LACMIP 332, San Pedro Sand). Los Angeles County Museum  
628 of Natural History.
- 629 Fricke, R., Eschmeyer, W., Van der Laan, R., 2018. Catalog of fishes: genera, species,  
630 references. California Academy of Sciences, San Francisco, CA, USA
- 631 Froese, R., Pauly, D., 2019. FishBase in the Catalogue of Life.
- 632 Gaither, M.R., Bowen, B.W., Rocha, L.A., Briggs, J.C., 2016. Fishes that rule the world:  
633 circumtropical distributions revisited. *Fish and Fisheries* 17, 664-679.  
634 <https://doi.org/10.1111/faf.12136>
- 635 González-Wevar, C.A., Nakano, T., Cañete, J.I., Poulin, E., 2010. Molecular phylogeny and  
636 historical biogeography of *Nacella* (Patellogastropoda: Nacellidae) in the Southern  
637 Ocean. *Molecular phylogenetics and evolution* 56, 115-124.  
638 <https://doi.org/10.1016/j.ympev.2010.02.001>
- 639 Grassle, J.F., 2000. The Ocean Biogeographic Information System (OBIS): an on-line,  
640 worldwide atlas for accessing, modeling and mapping marine biological data in a  
641 multidimensional geographic context. *Oceanography* 13, 5-7.
- 642 Heath, T.A., Huelsenbeck, J.P., Stadler, T., 2014. The fossilized birth–death process for  
643 coherent calibration of divergence-time estimates. *Proceedings of the National Academy*  
644 *of Sciences* 111, E2957-E2966. <https://doi.org/10.1073/pnas.1319091111>
- 645 Hoang, D.T., Chernomor, O., Von Haeseler, A., Minh, B.Q., Vinh, L.S., 2018. UFBoot2:  
646 improving the ultrafast bootstrap approximation. *Molecular biology and evolution* 35,  
647 518-522. <https://doi.org/10.1093/molbev/msx281>
- 648 Hopkins, D., Marincovich Jr, L., 1984. Whale biogeography and the history of the Arctic Basin.  
649 *Works of the Arctic Centre* 8, 7-24.
- 650 Hotaling, S., Foley, M.E., Lawrence, N.M., Bocanegra, J., Blanco, M.B., Rasoloarison, R.,  
651 Kappeler, P.M., Barrett, M.A., Yoder, A.D., Weisrock, D.W., 2016. Species discovery  
652 and validation in a cryptic radiation of endangered primates: coalescent-based species  
653 delimitation in Madagascar's mouse lemurs. *Molecular ecology* 25, 2029-2045.  
654 <https://doi.org/10.1111/mec.13604>
- 655 Jones, K.S., Weisrock, D.W., 2018. Genomic data reject the hypothesis of sympatric ecological  
656 speciation in a clade of *Desmognathus* salamanders. *Evolution* 72, 2378-2393.  
657 <https://doi.org/10.1111/evo.13606>

- 658 Kalyaanamoorthy, S., Minh, B.Q., Wong, T.K., von Haeseler, A., Jermini, L.S., 2017.  
659 ModelFinder: fast model selection for accurate phylogenetic estimates. *Nature Methods*  
660 14, 587-589. <https://doi.org/10.1038/nmeth.4285>
- 661 Kwun, H.J., Kim, J.-K., 2013. Molecular phylogeny and new classification of the genera  
662 Eulophias and Zoarchias (PISCES, Zoarcoidei). *Molecular Phylogenetics and Evolution*  
663 69, 787-795. <https://doi.org/10.1016/j.ympev.2013.06.025>
- 664 Landis, M.J., Matzke, N.J., Moore, B.R., Huelsenbeck, J.P., 2013. Bayesian analysis of  
665 biogeography when the number of areas is large. *Systematic Biology* 62, 789-804.  
666 <https://doi.org/10.1093/sysbio/syt040>
- 667 Lane, M.A., Edwards, J.L., 2007. The global biodiversity information facility (GBIF). *Biodiversity*  
668 *databases: Techniques, politics, and applications*, 1-4.
- 669 Machida, Y., Hashimoto, J., 2002. *Pyrolycus manusanus*, a new genus and species of deep-sea  
670 eelpout from a hydrothermal vent field in the Manus Basin, Papua New Guinea  
671 (Zoarcidae, Lycodinae). *Ichthyological Research* 49, 1-6.  
672 <https://doi.org/10.1007/s102280200000>
- 673 Marinovich, L., Gladenkov, A.Y., 1999. Evidence for an early opening of the Bering Strait.  
674 *Nature* 397, 149-151. <https://doi.org/10.1038/16446>
- 675 Matschiner, M., Hanel, R., Salzburger, W., 2011. On the origin and trigger of the notothenioid  
676 adaptive radiation. *PloS one* 6, e18911. <https://doi.org/10.1371/journal.pone.0018911>
- 677 Matzke, N.J., 2013. Probabilistic historical biogeography: new models for founder-event  
678 speciation, imperfect detection, and fossils allow improved accuracy and model-testing.  
679 *Frontiers of Biogeography* 5. <https://doi.org/10.21425/F5FBG19694>
- 680 Matzke, N.J., 2014. Model selection in historical biogeography reveals that founder-event  
681 speciation is a crucial process in island clades. *Systematic Biology* 63, 951-970.  
682 <https://doi.org/10.1093/sysbio/syu056>
- 683 Møller, P.R., Nielsen, J.G., Anderson, M.E., 2005. Systematics of polar fishes. *Fish Physiology*  
684 22, 25-78. [https://doi.org/10.1016/S1546-5098\(04\)22002-7](https://doi.org/10.1016/S1546-5098(04)22002-7)
- 685 Nauheimer, L., Metzler, D., Renner, S.S., 2012. Global history of the ancient monocot family  
686 Araceae inferred with models accounting for past continental positions and previous  
687 ranges based on fossils. *New Phytologist* 195, 938-950. <https://doi.org/10.1111/j.1469-8137.2012.04220.x>
- 688
- 689 Nazarkin, M., 1998. New stichaeid fishes (Stichaeidae, Perciformes) from Miocene of Sakhalin.  
690 *Journal of Ichthyology* 38, 279-291.

- 691 Nazarkin, M., 2002. Gunnels (Perciformes, Pholidae) from the Miocene of Sakhaline Island.  
692 *Journal of Ichthyology* 42, 279-288.
- 693 Nazarkin, M., Yabumoto, Y., 2015. New fossils of Neogene pricklybacks (Actinopterygii:  
694 Stichaeidae) from East Asia. *Zoosystematica Rossica* 24, 128-137.
- 695 Near, T.J., Dornburg, A., Harrington, R.C., Oliveira, C., Pietsch, T.W., Thacker, C.E., Satoh,  
696 T.P., Katayama, E., Wainwright, P.C., Eastman, J.T., 2015. Identification of the  
697 notothenioid sister lineage illuminates the biogeographic history of an Antarctic adaptive  
698 radiation. *BMC evolutionary biology* 15, 109. <https://doi.org/10.1186/s12862-015-0362-9>
- 699 Near, T.J., Dornburg, A., Kuhn, K.L., Eastman, J.T., Pennington, J.N., Patarnello, T., Zane, L.,  
700 Fernández, D.A., Jones, C.D., 2012. Ancient climate change, antifreeze, and the  
701 evolutionary diversification of Antarctic fishes. *Proceedings of the National Academy of*  
702 *Sciences* 109, 3434-3439. <https://doi.org/10.1073/pnas.1115169109>
- 703 Nguyen, L.-T., Schmidt, H.A., Von Haeseler, A., Minh, B.Q., 2015. IQ-TREE: a fast and effective  
704 stochastic algorithm for estimating maximum-likelihood phylogenies. *Molecular biology*  
705 *and evolution* 32, 268-274. <https://doi.org/10.1093/molbev/msu300>
- 706 Orr, J.W., Spies, I., Stevenson, D.E., Longo, G.C., Kai, Y., Ghods, S., Hollowed, M., 2019.  
707 Molecular phylogenetics of snailfishes (Cottoidei: Liparidae) based on MtDNA and  
708 RADseq genomic analyses, with comments on selected morphological characters.  
709 *Zootaxa* 4642, 1-79. <https://doi.org/10.1016/j.ympev.2004.06.015>
- 710 Paradis, E., Schliep, K., 2019. ape 5.0: an environment for modern phylogenetics and  
711 evolutionary analyses in R. *Bioinformatics* 35, 526-528.  
712 <https://doi.org/10.1093/bioinformatics/bty633>
- 713 Quinlan, A.R., Hall, I.M., 2010. BEDTools: a flexible suite of utilities for comparing genomic  
714 features. *Bioinformatics* 26, 841-842. <https://doi.org/10.1093/bioinformatics/btq033>
- 715 Rabosky, D.L., Chang, J., Title, P.O., Cowman, P.F., Sallan, L., Friedman, M., Kaschner, K.,  
716 Garilao, C., Near, T.J., Coll, M., 2018. An inverse latitudinal gradient in speciation rate  
717 for marine fishes. *Nature* 559, 392-395. <https://doi.org/10.1038/s41586-018-0273-1>
- 718 Radchenko, O., 2016. Timeline of the evolution of eelpouts from the suborder Zoarcoidei  
719 (Perciformes) based on DNA variability. *Journal of Ichthyology* 56, 556-568.  
720 <https://doi.org/10.1134/S0032945216040123>
- 721 Radchenko, O.A., 2015. The System of the Suborder Zoarcoidei (Pisces, Perciformes) as  
722 Inferred from Molecular Genetic Data. *Russian Journal of Genetics* 51, 1273-1290.  
723 <https://doi.org/10.1134/S1022795415100130>

- 724 Ree, R.H., 2005. Detecting the historical signature of key innovations using stochastic models of  
725 character evolution and cladogenesis. *Evolution* 59, 257-265.  
726 <https://doi.org/10.1111/j.0014-3820.2005.tb00986.x>
- 727 Ree, R.H., Smith, S.A., 2008. Maximum likelihood inference of geographic range evolution by  
728 dispersal, local extinction, and cladogenesis. *Systematic Biology* 57, 4-14.  
729 <https://doi.org/10.1080/10635150701883881>
- 730 Revell, L.J., 2012. phytools: an R package for phylogenetic comparative biology (and other  
731 things). *Methods in Ecology and Evolution* 3, 217-223. [https://doi.org/10.1111/j.2041-](https://doi.org/10.1111/j.2041-210X.2011.00169.x)  
732 [210X.2011.00169.x](https://doi.org/10.1111/j.2041-210X.2011.00169.x)
- 733 Ronquist, F., 1997. Dispersal-vicariance analysis: a new approach to the quantification of  
734 historical biogeography. *Systematic Biology* 46, 195-203.  
735 <https://doi.org/10.1093/sysbio/46.1.195>
- 736 Ronquist, F., Teslenko, M., Van Der Mark, P., Ayres, D.L., Darling, A., Höhna, S., Larget, B.,  
737 Liu, L., Suchard, M.A., Huelsenbeck, J.P., 2012. MrBayes 3.2: efficient Bayesian  
738 phylogenetic inference and model choice across a large model space. *Systematic*  
739 *biology* 61, 539-542. <https://doi.org/10.1093/sysbio/sys029>
- 740 Schluter, D., 2000. *The ecology of adaptive radiation*. OUP Oxford.
- 741 Shmidt, P., 1950. Ryby Okhotskogo Morya [Fishes of the Sea of Okhotsk]. *Trudy*  
742 *Tikhookeanskogo Komiteta* 6, 1-370.
- 743 Suyama, M., Torrents, D., Bork, P., 2006. PAL2NAL: robust conversion of protein sequence  
744 alignments into the corresponding codon alignments. *Nucleic acids research* 34, W609-  
745 W612. <https://doi.org/10.1093/nar/gkl315>
- 746 Yabumoto, Y., Uyeno, T., 1994. Late Mesozoic and Cenozoic fish faunas of Japan. *Island Arc* 3,  
747 255-269. <https://doi.org/10.1111/j.1440-1738.1994.tb00115.x>
- 748 Zhang, C., Stadler, T., Klopstein, S., Heath, T.A., Ronquist, F., 2016. Total-evidence dating  
749 under the fossilized birth–death process. *Systematic Biology* 65, 228-249.  
750 <https://doi.org/10.1093/sysbio/syv080>  
751